IEEE Access
Multidisciplinary | Rapid Review | Open Access Journal

Received 14 May 2023, accepted 11 June 2023, date of publication 16 June 2023, date of current version 22 June 2023.

Digital Object Identifier 10.1109/ACCESS.2023.3286886

RESEARCH ARTICLE

Robust Underwater Acoustic Communication Using the Overlapped Chirp Spread Carrier Technique in Doubly Spread Environments

CHANG-HYUN YOUN, HYUNG-IN RA, KYUNG-WON LEE, AND KI-MAN KIM
Department of Radio Communication Engineering, Korea Maritime and Ocean University, Yeongdo-gu, Busan 49112, South Korea
Corresponding author: Ki-Man Kim (kimkim@kmou.ac.kr)

ABSTRACT The performance of underwater acoustic communication is significantly affected by multipath propagation and Doppler spread. In this paper, we propose a new communication technique called overlapped chirp spread carrier (OCSC) by modifying the existing sweep spread carrier (SSC) technique, which is robust in a multipath propagation environment. Our proposed OCSC technique uses a repeated carrier wave by combining up-chirp and down-chirp signals and estimates and corrects the Doppler shift frequency of the received signal by utilizing the characteristics of the correlation function of each up-chirp and down-chirp. To demonstrate the performance of the proposed OCSC technique, we provide the results of a simulation using an underwater channel simulator and sea trial conducted in the East Sea. As a result of the sea trial, when demodulating using only the estimated Doppler shift frequency, the uncoded bit error rate reached 0.135. However, when our proposed correction method was applied to the estimated Doppler frequency, the uncoded bit error rate decreased to 0.001.

INDEX TERMS Bit error rate, multipath propagation, Doppler spread, overlapped chirp spread carrier, sea trial, underwater acoustic communication.

I. INTRODUCTION

Underwater acoustic communication is used in various applications, such as underwater navigation, underwater vehicles, underwater sensor networks, marine environment monitoring, and military purposes [1], [2], [3], [4], [5], [6], [7]. However, unlike radio frequency (RF) communication, underwater acoustic communication has many obstacles, such as high propagation loss, frequency selective fading, narrow bandwidth, and fast time variability [8], [9], [10]. The speed of the sound wave changes according to the depth, salinity, and temperature of the water, and the movement path of the sound wave changes due to refraction [11]. In addition, as sound waves are transmitted, there are problems; these include multipath propagation by the seafloor or sea level and the Doppler shift effect caused by the movement of wind, ocean currents, and transceivers [12], [13]. Especially in shallow water environments where the depth is not deep, multipath propagation is the main problem and degrades the performance because it causes ISI (Inter Symbol Interference) due to its long delay time. Many studies have been conducted on spread spectrum techniques with less affected modulation methods in this type of multipath propagation environment [14], [15], [16], [17].

Spread spectrum techniques are methods of spreading and transmitting the bandwidth of the signal widely and include frequency hopping spread spectrum (FHSS), direct sequence spread spectrum (DSSS), and chirp spread spectrum (CSS) [18]. FHSS is a technique that involves dividing the entire bandwidth and transmitting information using a hopping code, whereby the frequency is changed over time. This method is particularly effective in environments where a Doppler frequency is present, but it only uses a partial amount of the energy in the transmitted signal, causing it to be vulnerable in environments with a low signal-to-noise ratio (SNR) [19]. DSSS assigns a pseudo-noise sequence to

The associate editor coordinating the review of this manuscript and approving it for publication was Qilian Liang.

This work is licensed under a Creative Commons Attribution-NonCommercial-NoDerivatives 4.0 License.
For more information, see https://creativecommons.org/licenses/by-nc-nd/4.0/

each symbol to spread the signal across the bandwidth. DSSS is highly resilient in environments with low SNR, with advantages of power and bandwidth efficiency for long-distance communication when compared to FHSS. However, DSSS is highly sensitive to Doppler frequency variability and requires complex synchronization at the receiving end, which can be a significant disadvantage [20]. CSS is a spread spectrum technique that addresses the limitations of SNR and Doppler frequency sensitivity found in the previously mentioned spread spectrum techniques. In this technique, symbols are composed of linear frequency modulation (LFM) signals, where the frequency changes linearly with time. CSS is designed to overcome the disadvantages of FHSS and DSSS and is a more robust spread spectrum technique [21].

Based on the study of these CSS signals, Lee et al. [22] applied a differential coding method; the size of the matched filter was doubled, and the performance was improved by taking advantage of the fact that the time-bandwidth product cost increases. Azim et al. [23] proposed dual-mode chirp spread spectrum (DM-CSS) modulation for low-power wide-area networks. DM-CSS achieved higher spectral efficiency than other models, such as long-range modulation. Zhu et al. [24] proposed an orthogonal chirp division multiplexing (OCDM) method that used a chirp signal for carrier modulation; under multipath propagation conditions where the delay spread was longer than the guard interval, the conventional orthogonal frequency out-performed the orthogonal frequency division multiplexing (OFDM). Kebkal and Bannasch [25] proposed an SSC (sweep spread carrier) technique using a periodically repeated up-chirp signal as a carrier. Unlike the conventional CSS technique, the SSC technique transmitted a chirp signal as a carrier signal rather than information. This technique separated multipath arrival by converting it into frequency at the receiving end according to the absolute value of the time delay according to multipath propagation.

In underwater acoustic communication, due to the environmental characteristics, Doppler shift frequency occurs due to waves, wind, ocean current, and the mobility of the transceiver. This causes the deterioration of communication performance; thus, to improve communication performance, it is essential to compensate for the distortion caused by the Doppler shift effect. Techniques for estimating the Doppler shift frequency of the received signal have been greatly studied [26], [27]. In general, a communication packet transmits a preamble signal at the beginning of a data section that transmits information, and the preamble signal indicates the exact starting point of a data frame. In addition to finding the starting point, the approximate Doppler shift frequency of the data frame can be determined using the Doppler bank [28]. However, when the Doppler bank method is applied, the number of matched filters is increased to increase the accuracy of the Doppler shift frequency estimation value; thus, there is a disadvantage in the large amount of calculations needed at the receiving end.

In this paper, we propose an overlapping chirp spread carrier (OCSC) technique that uses a signal in which a periodically repeated up-chirp signal and a down-chirp signal are combined as a carrier frequency by modifying the existing SSC technique. Compared to the existing SSC method, this method increases the transmission rate because it can transmit phase-modulated pulses to each of the up-chirp and down-chirp signals, and it is also robust in a multipath transmission environment. In addition, the Doppler shift frequency can be estimated through the chirp signal and the cross-correlation function. However, errors can be included in the estimated Doppler shift frequencies, and a correction method for these errors is presented. Moreover, the results of simulations and sea trials using the proposed OCSC technique are presented.

The remainder of this paper proceeds as follows: Section II explains the existing SSC method; Section III elucidates the proposed OCSC method and the concept of Doppler shift frequency estimation and correction; Section IV describes the simulation results based on the bellhop model using the estimated Doppler shift frequency and presents the results in terms of the bit error rate; Section V examines the results from sea experiments; and Section VI provides the conclusion.

II. TRADITIONAL SSC TECHNIQUE

The SSC technique is a communication method that uses only continuous up-chirp signals as carrier waves to transmit phase-modulated pulses. Since this technique has robust characteristics in a multipath propagation environment, it has an advantage of overcoming an ISI that arises in these conditions.

The SSC signal utilizes a periodic up-chirp signal, which sweeps from the minimum frequency f_{min} to the maximum frequency f_{max}, as the carrier during the sweep time of T_s. The SSC signal is described by the following equation:

$$c^{up}(t) = A_c \exp\left[j2\pi\left(f_{min}\tau(t) + k\tau(t)^2\right)\right] \tag{1}$$

where A_c is the amplitude of the signal, $k = (f_{max} - f_{min})/2T_S$ and is a coefficient representing the rising frequency variation rate, $\tau(t) = t - T_S\left\lfloor \frac{t}{T_S} \right\rfloor$ and is a continuous chirp-shaped periodic sweep with cycle duration T_S.

The term $\left\lfloor {}^{t}/_{T_S} \right\rfloor$ is defined as the final integer not greater than ${}^{t}/_{T_S}$, where N is the number of chirp pulses that compose the carrier waveform, and $T_C = NT_S$ is the overall carrier time. Fig. 1 shows the concept of the SSC method in the time-frequency domain.

A signal encoded by phase shift keying (PSK) is represented as follows:

$$s^{up}(t) = \sum_{n=-\infty}^{\infty} A_s exp\left[jD_n p(t - nT)\right] \tag{2}$$

where A_s represents the amplitude of the signal, and $p(t)$ is a pulse for phase modulation. D_n is the phase encoded data symbol being communicated, and T is the signal interval.

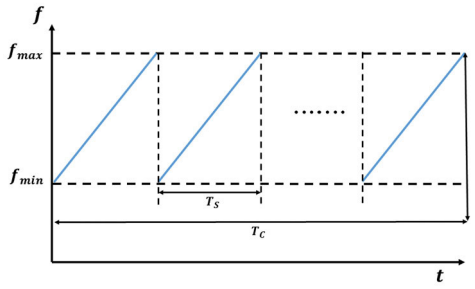

FIGURE 1. Concept of the SSC modulation [25].

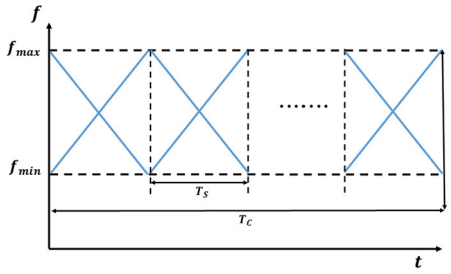

FIGURE 2. Concept of the OCSC modulation.

After being modulated onto the carrier, the signal transmitted over the channel is expressed as follows:

$$x(t) = Re[s^{up}(t)\, c^{up}(t)] \tag{3}$$

III. PROPOSED OCSC TECHNIQUE

A. OCSC SIGNAL

The OCSC technique is an extension of the existing SSC technique. In contrast to the SSC technique, which uses only the up-chirp signal as the carrier, the OCSC technique combines and repeats both the up-chirp and down-chirp signals with a constant symbol period, as shown in Fig. 2. Furthermore, the OCSC technique transmits binary modulated pulses for each up-chirp and down-chirp, leading to a doubled transmission speed compared to the SSC technique. The OCSC technique is described in (4).

$$x(t) = Re\left[s^{up}(t)\, c^{up}(t) + s^{down}(t)\, c^{down}(t)\right] \tag{4}$$

where $s(t)$ means up-chirp and down-chirp phase-modulated pulses, and $c^{down}(t)$ means down-chirp carrier. The expression describing $c^{down}(t)$ is shown in (5).

$$c^{down}(t) = A_c exp\left[j2\pi\left(f_{max}\tau(t) + w\tau(t)^2\right)\right] \tag{5}$$

where, $w = (f_{min} - f_{max})/2T_S$ and is a coefficient representing the falling frequency variation rate.

B. DOPPLER SHIFT FREQUENCY ESTIMATION IN OCSC MODULATION

To estimate the Doppler frequency, the cross-correlation function is calculated between each symbol, and the peak position is identified. The amount of change in the interval between the identified peaks is then used to estimate the Doppler frequency. The OCSC is a form in which up-chirp and down-chirp signals are combined for each symbol. Therefore, if the up-chirp matched filter and down-chirp matched filter are applied alternately for each symbol, the peak point for the up-chirp and the peak point for the down-chirp appear for each symbol, and the Doppler frequency can then be estimated by measuring the amount of change between the peak points for the up-chirps and down-chirps.

The variables T_{up} and T_{down} represent the times at which the matched filtering maximum appears in the up-chirp and down-chirp, respectively. When the OCSC signal has a Doppler shift frequency of 0 Hz, the time interval T_s can be calculated as follows:

$$T_s = T_{down}(i) - T_{up}(i) \tag{6}$$

where i means the index of the up and down chirp peaks. If there is a Doppler shift, the time interval T_s between T_{up} and T_{down} has a variation of Δ because the signal is compressed or expanded. It is expressed as follows:

$$T_{down}(i) - T_{up}(i) = T_s + \Delta(i) \tag{7}$$

The Doppler shift frequency (f_d) can be estimated by utilizing the variation value Δ. Specifically, when the up and down peaks are paired, the Doppler shift frequency estimation can be expressed as follows:

$$f_d(i) = \frac{(f_{min} - f_{max}) \times \Delta(i)}{2T_s} \tag{8}$$

Since the number of Doppler shift frequencies estimated from the received OCSC signal is N/2, the Doppler shift frequency of the entire OCSC signal can be expressed as follows via rearrangements with (7) and (8):

$$\hat{f_d} = \frac{1}{N/2}\sum[\frac{(f_{min} - f_{max}) \times \left(T_{down}(i) - T_{up}(i) - T_s\right)}{2T_s}] \tag{9}$$

Finally, to estimate the Doppler shift frequency of the OCSC signal, the estimated Doppler shift frequencies are averaged. Fig. 3 illustrates the process for estimating the Doppler shift frequency of the OCSC signal.

C. DOPPLER SHIFT FREQUENCY CORRECTION

The estimation of the Doppler shift frequency using the correlation function between the up-chirp and down-chirp is prone to error due to decreased correlation characteristics between the OCSC signal and the chirp signal during pulse synthesis. When the OCSC signal experiences a Doppler shift, the chirp-sweep time of the signal changes, leading to a reduction in the correlation characteristics with the chirp signal. Therefore, in this paper, the effect of the Doppler shift frequency estimated using the OCSC signal and its correction were verified through simulation.

Initially, while changing the amount of data in the OCSC signal, that is, the number of symbols, to 500, 1000, 2000, 3000, 5000, and 10000, the relative error aspect of the

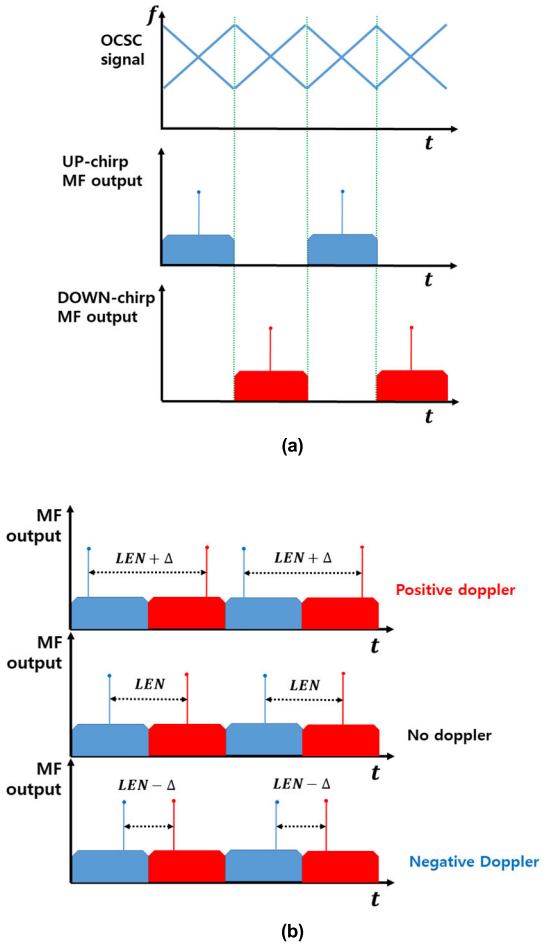

FIGURE 3. Process of estimating the OCSC signal Doppler shift frequency. (a) Application of matched filtering to the OCSC signal, (b) Doppler shift effect on the positive Doppler and negative Doppler.

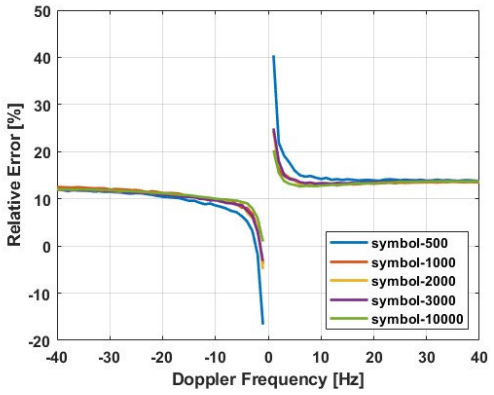

FIGURE 4. Relative error of the Doppler frequency using the OCSC method.

Doppler shift frequency estimation value was confirmed through simulation. As shown in Fig. 4, the relative error patterns were similar. Therefore, it was confirmed that our method proposed could be applied regardless of the amount of information. Here, the error increased significantly

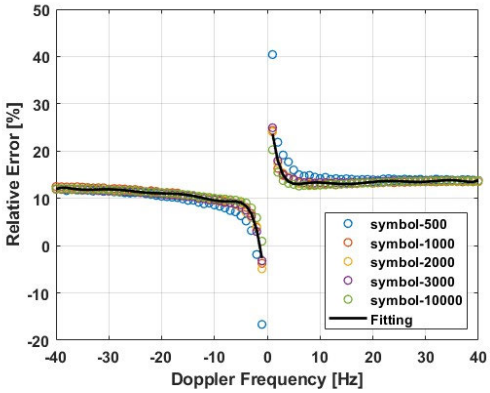

FIGURE 5. Polynomial equation plotting for error appearance using nonlinear LS fitting.

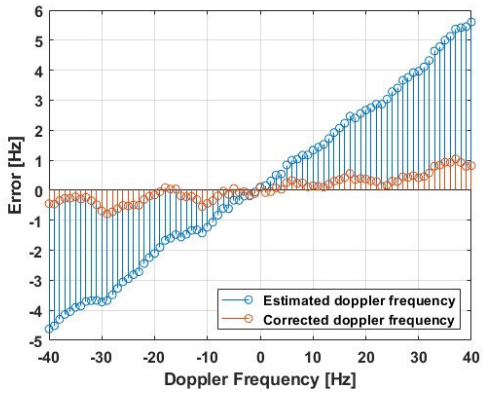

FIGURE 6. Comparison of the error with the estimated and corrected Doppler frequency.

around the Doppler shift frequency 0 and was determined by calculating the error shown on the axis in the form of [(B-A)/B] × 100, where A is the estimated Doppler shift frequency and B is the actual Doppler shift frequency. Since the error is a number and the denominator is a small value close to 0, the relative error value appeared large, but the difference between the estimated Doppler shift frequency and the actual Doppler shift frequency was a very low value.

Next, to generalize the relative error patterns, each case of positive Doppler and negative Doppler was represented in polynomial form using nonlinear least square curve fitting (Fig. 5). Finally, the estimated Doppler shift frequency is corrected by substituting the estimated Doppler shift frequency into the polynomial derived by fitting the nonlinear least squares (LS) curve to compensate for the errors.

A simulation was conducted to validate the effectiveness of the proposed Doppler shift frequency correction method. The OCSC signal was set to have a data amount of 1,000 bits, T_s was 10 ms, and SNR of −3 dB. Doppler shift frequencies ranging from −40 Hz to +40 Hz were used for the simulation. The simulation results are shown in Fig. 6, where the x-axis represents the virtually generated Doppler shift frequency, and the y-axis represents the error between the virtually

TABLE 1. Simulation parameters.

PARAMETER	VALUE
Sampling frequency	192 kHz
Carrier frequency	11 kHz
Data rate	100 bps
Bandwidth	2 kHz
Sweep time	10 ms
SNR	-10, -5 , 0 dB
Doppler shift frequency	-40 ~ 40 Hz

generated Doppler shift frequency and the estimated Doppler shift frequency.

The blue value represents the estimated Doppler shift frequency error, while the red value represents the corrected Doppler shift frequency error. From the correction of the Doppler shift frequency using the estimated Doppler shift frequency, an error of less than approximately 1 Hz was obtained

IV. SIMULATIONS AND RESULTS

The performance of the OCSC method under multipath propagation and Doppler channel conditions was evaluated using the bellhop model-based VirTEX simulator [29]. The simulation was conducted using actual sound speed data from the West Sea of South Korea, representing a shallow sea environment, and from the East Sea of South Korea, representing a deep water environment. No separate error correction technique was applied to the generated communication signal. The parameters applied to the simulation are shown in Table 1.

A. SHALLOW WATER CHANNEL

Shallow water environments are prone to multipath propagation because the water depth is not deep. Fig. 7(a) shows the sound speed distribution in the West Sea applied to the simulation. In the simulation, it is assumed that the transmission distance between the transmitter and receiver is 100 m, the water depth is 20 m, and the depths of the transmitter and receiver are approximately 5 m and 15 m, respectively. Fig. 7(b) shows the ray tracing, and the channel impulse response is shown in Fig. 7(c).

Fig. 8 shows the simulation results according to the SNR. In the figure, red data represents the result at 0 dB, green at −5 dB, and black at −10 dB. Fig. 8(a) shows the respective errors according to the estimated Doppler shift frequency and the corrected Doppler shift frequency. The error of the estimated Doppler shift frequency indicated by '×' increased as the given Doppler shift frequency increased regardless of the value of SNR, but the error of the corrected Doppler shift frequency indicated by '◯' remarkably low.

Fig. 8(b) shows the result from the uncoded bit error rate using the estimated Doppler shift frequency and the corrected Doppler shift frequency at various SNR. In the figure,

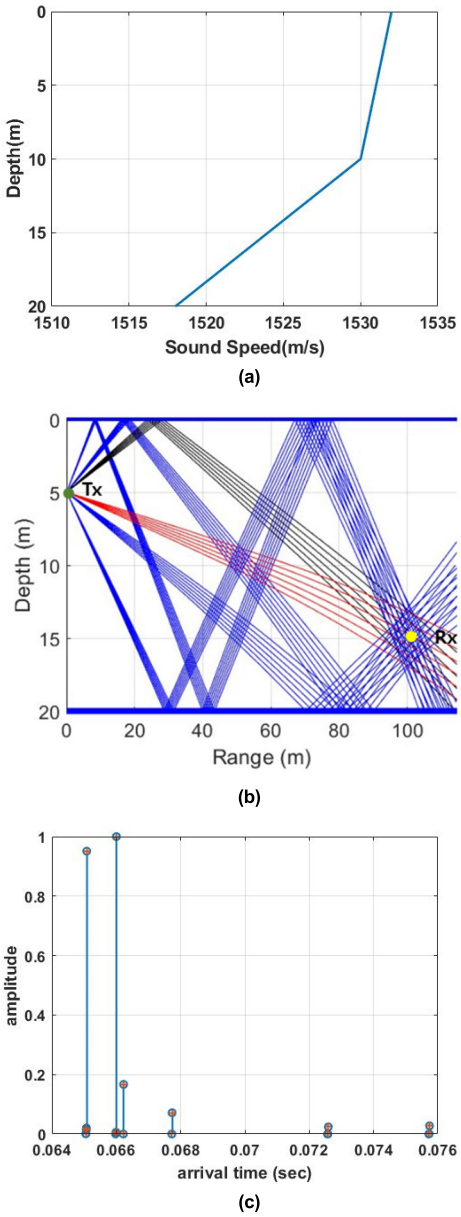

FIGURE 7. Shallow water channel using the VirTEX simulator. (a) Sound speed profile, (b) Ray tracing, (c) Channel impulse response.

'□' represents the bit error rate when the Doppler shift frequency is not compensated.

When the Doppler value is small, the data are demodulated, but when the Doppler value changes even slightly, the data are not demodulated. '×' represent the bit error rate when compensated with the estimated Doppler shift frequency.

When the Doppler value is within ±10 Hz, the data are demodulated, and when it is higher than 10 Hz, the error rate increases. Finally, '◯' represent the bit error rate when compensated with our corrected Doppler shift frequency method. Most of the data demodulation is accurate in all sections. Therefore, the performance is improved by correcting the estimated Doppler shift frequency.

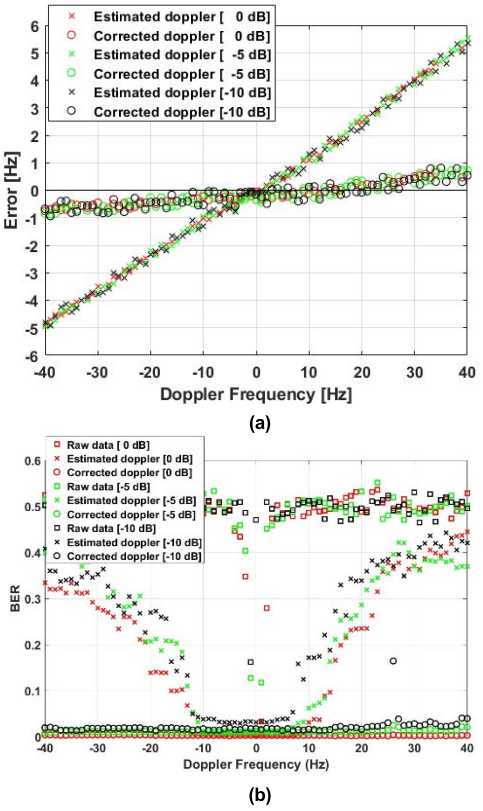

FIGURE 8. Results from passing through the VirTEX West sea channel. (a) Estimated Doppler frequency error and (b) Uncoded BER.

B. DEEP WATER CHANNEL

In the deep water environment, even if multipath exists in the received signal, there is a relatively long delay time due to the deep water depth, unlike the shallow sea environment. Fig. 9(a) shows the sound speed distribution in the East Sea applied to the simulation. In the simulation, it is assumed that the transmission distance between the transmitter and receiver is 5 km, the water depth is 1,000 m, and the depths of the transmitter and receiver are approximately 200 m and 300 m, respectively. In Fig. 9(c), multipath propagation appears after approximately 140 ms.

Fig. 10 represents the result of passing through the deep water channel. Similar to Fig. 8, Fig. 10(a) confirms that the error of the corrected Doppler frequency is significantly lower than that of the estimated Doppler frequency. Fig. 10(b) shows the uncoded bit error rate using the estimated and corrected Doppler frequencies.

When compensated with the estimated Doppler frequency, the data can be demodulated when the Doppler value is within 10 Hz, but the error rate increases when the value is higher than that. However, when the corrected Doppler frequency is compensated, the data can be demodulated in all sections.

Table 2 compares the calculation time and error between the Doppler shift frequency estimation and correction method using the proposed OCSC technique and the Doppler shift frequency estimation method, which is one of the existing

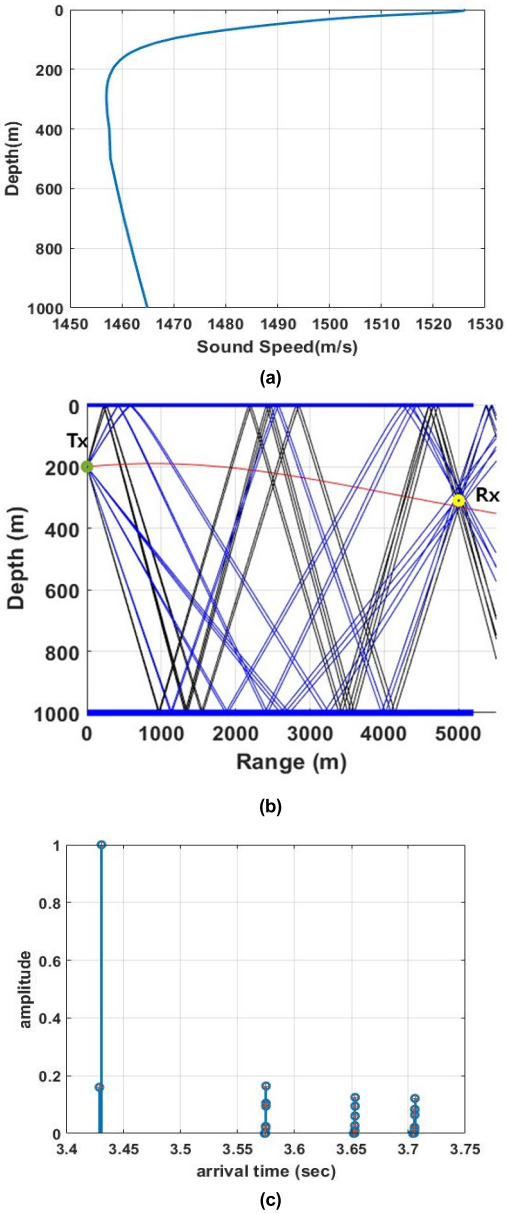

FIGURE 9. Deep water channel using the VirTEX simulator. (a) Sound speed profile, (b) Ray tracing and (c) Channel impulse response.

Doppler shift frequency estimation methods. Here, the error was obtained as the root mean square (RMS) of the difference between the actual Doppler value and the estimated Doppler value. Although the processing time varies depending on the resolution of the Doppler bank, in this simulation, the resolution of the Doppler bank was set to 0.2 Hz.

When comparing Doppler bank method and the proposed method, there is no difference in the error rate of the compensated data when Doppler frequency correction is performed. However, the Doppler bank method has a disadvantage that the computation time greatly increases according to the resolution, but the proposed method has the

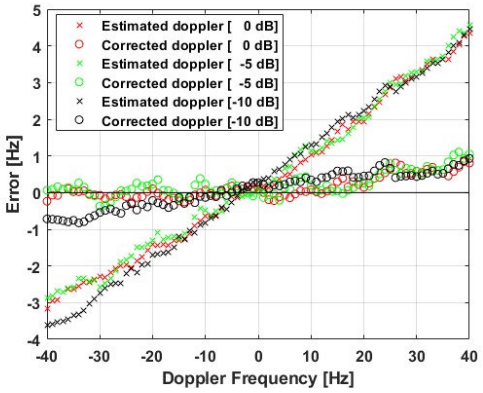

(a)

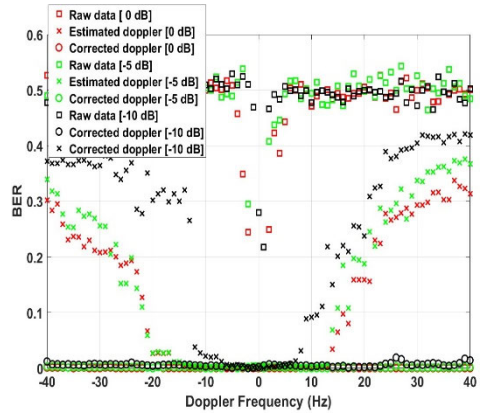

(b)

FIGURE 10. Result from passing through the VirTEX East sea channel. (a) Estimated Doppler frequency error and (b) uncoded BER.

TABLE 2. Program operation time and performance according to each method.

Case	Operation time	RMS error
Doppler bank	5.943 s	0.022
Proposed doppler estimation	3.891 s	1.997
Proposed doppler estimation and correction	3.938 s	0.346

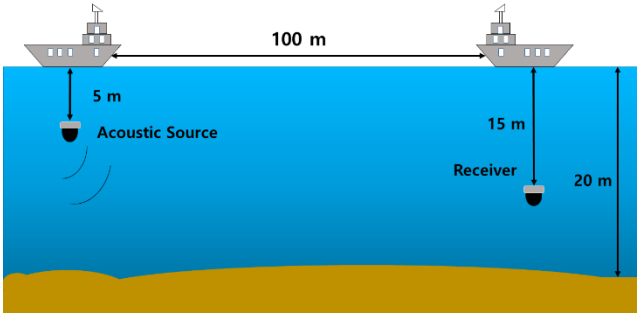

FIGURE 11. Schematic of the sea trial.

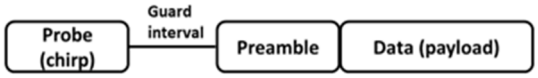

FIGURE 12. Packet structure.

advantage of a smaller computation amount than the Doppler bank method. The time calculated in the simulation was measured using Matlab's built-in functions 'tic' and 'toc', and the specifications of the computer used were Intel Core i7-7700K/4.20 GHz CPU/RAM: 32 GB.

V. SEA TRIAL AND RESULTS

A. EXPERIMENTAL ENVIRONMENT

An offshore sea trial was conducted near Pohang, South Korea, in March 2023, to verify the performance of our proposed method. However, due to poor weather conditions at the time of the trial, a rather high wave height of approximately 3 m was measured. Consequently, the transmission distance was set to 100 m. The water depth at the test point was approximately 20 m, with the transmitter water depth and receiver water depth being 5 m and 15 m, respectively, based on sea level. A schematic diagram of the marine experiment is depicted in Fig. 11.

In the trial, the ITC-1007 model was used as the projector, and the signal was designed to consider the transmission characteristics of this projector. The OCSC signal had a center frequency of 11 kHz, a bandwidth of 2 kHz, a sweep time of 10 ms, and a transmission rate of 200 bps with a total of 1,000 bits transmitted. Virtual Doppler was inserted into the transmission signal due to the inability to configure the actual Doppler channel environment caused by weather conditions. The virtual Doppler was transmitted at 10 Hz intervals ranging from −40 Hz to 40 Hz.

The symbols of the OCSC signal were binary PSK modulated, and pulse shaping was performed using a raised cosine filter with a roll-off coefficient of 0.5. The packet of the transmitted signal is shown in Fig. 12 and was accordingly configured.

To determine the starting point of the received signal, a chirp signal with a duration of 1 second was transmitted, and a guard interval of 0.5 seconds was inserted between the probe signal and the preamble signal. The preamble signal was transmitted before the data period to accurately synchronize the data frame. For the preamble signal, a total of 510 bits were transmitted by repeating an m-sequence of 255 bits twice consecutively using binary PSK modulation. Thus, the length of one packet of the OCSC signal was approximately 7.5 seconds.

B. CHANNEL CHARACTERISTICS

To assess the transmission characteristics of the channel, the LFM signal was repeatedly transmitted. The carrier

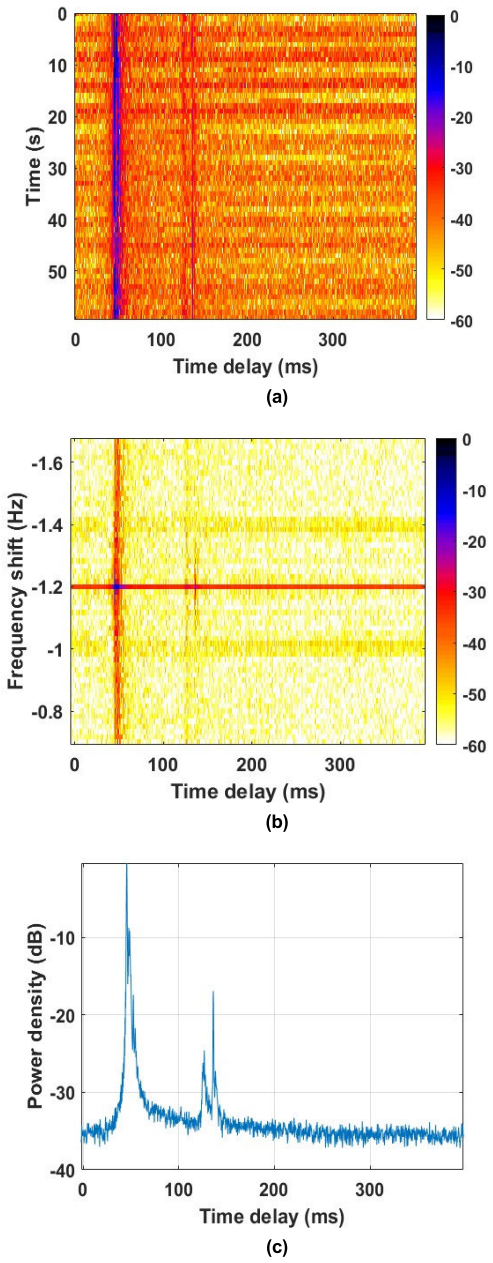

FIGURE 13. Underwater channel characteristics in sea trial. (a) Channel impulse response, (b) Delay-Doppler spread function, and (c) Power delay profile.

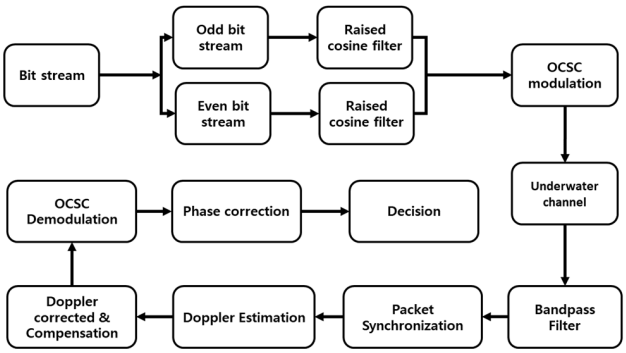

FIGURE 14. Block diagram of OCSC transmission.

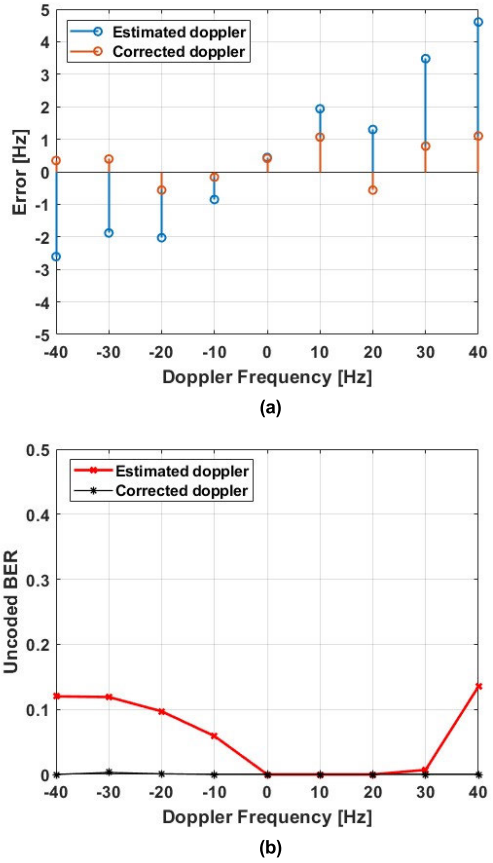

FIGURE 15. Results of a sea trial. (a) Estimated Doppler frequency error and (b) uncoded BER.

frequency of the LFM signal was 11 kHz, the bandwidth was 2 kHz, the ping interval was 1 s, and the ping length was 50 ms. The channel characteristics were measured and are shown in Fig. 13. Although the experiment was conducted in a stationary trial, it was estimated that the transceiver terminal's movement due to the influence of the ocean current caused a Doppler frequency shift of approximately −1.2 Hz.

The power delay profile of the channel is shown in Fig. 13(c). Multipaths were observed with a time difference of approximately 2 ms based on the direct path, multipaths after approximately 90 ms were observed, and the magnitude difference was more than 17 dB compared to the direct path. The impact was determined to be insignificant.

C. SEA TRIAL RESULTS

The OCSC signal was subjected to data modulation and demodulation in the order shown in Figure 14. In the transmitter, odd and even bits were separated from the transmission bit string, and a raised cosine filter was applied to shape the pulse train. The pulse train was then transmitted via OCSC modulation using up-chirp and down-chirp.

The received signal, after passing through the channel, first underwent bandpass filtering to remove unnecessary frequency components, and then frame synchronization was performed. The Doppler shift frequency was estimated using the previously proposed technique, corrected again, and the received signal's Doppler shift frequency was compensated. The OCSC signal was then demodulated, and phase correction was performed using a phase-locked loop (PLL). Finally, the data were demodulated.

The results of the communication test are presented in Fig. 15. Fig. 15(a) shows the errors of virtual Doppler, estimated Doppler, and corrected Doppler. In Fig. 15(b), the red line represents the estimated Doppler shift frequency, while the black line represents the uncoded bit error rate with corrected Doppler shift frequency compensation. Although the virtual Doppler shift frequency used in the trial ranged from −40 Hz to 40 Hz, the actual Doppler shift was affected by ocean currents, resulting in an error between the virtual Doppler shift frequency and the relatively estimated and corrected Doppler shift frequencies. As a result, the BER of the Doppler estimation method was asymmetric at positive and negative Doppler values. However, in the proposed Doppler correction method, most of the BER values were zero.

VI. CONCLUSION

Underwater acoustic communication has the heavy time spread by multipath and Doppler spreads. In this paper, an OCSC method of underwater acoustic communication is proposed to improve the performance of the SSC method using a chirp signal as a carrier. In our proposed method, carriers combined with up-chirp and down-chirp signals are used to double the transmission rate compared to the conventional SSC method. The Doppler shift frequency is estimated through the cross-correlation function of the up-chirps and down-chirps, and then it is corrected. To confirm the performance of our proposed method, simulations and sea trials were performed, and the results were provided. In the simulation, the proposed Doppler transition frequency estimation and correction were compared in terms of performance and calculation time with the existing Doppler transition frequency estimation method, and the proposed OCSC technique performed better in terms of calculation time than the existing Doppler bank method. In the trial, the virtual Doppler shift frequency was included in the transmission signal and transmitted to assess the performance of our Doppler shift frequency estimation and our proposed correction method. As a result of the sea trial, when the estimated Doppler shift frequency was compensated, the uncoded bit error rate ranged from a minimum of 0 to a maximum of 0.135; however, when the estimated Doppler shift frequency was corrected and compensated, the majority of the results were 0. In the future, research on the change in the transmission method according to the change in the channel environment is needed that includes sea trials in the actual Doppler shift environment.

REFERENCES

[1] S. Climent, A. Sanchez, J. Capella, N. Meratnia, and J. Serrano, "Underwater acoustic wireless sensor networks: Advances and future trends in physical, MAC and routing layers," *Sensors*, vol. 14, no. 1, pp. 795–833, Jan. 2014.
[2] Y. Yao, Y. Wu, M. Zhu, D. Li, and J. Tao, "Efficient on-off keying underwater acoustic communication for seafloor observation networks," *Appl. Sci.*, vol. 10, no. 6, p. 1986, Mar. 2020.
[3] E. T. Michailidis, G. Tuna, G. Gezer, S. M. Potirakis, and K. Gulez, "ANN-based control of a multiboat group for the deployment of an underwater sensor network," *Int. Jounal Distrib. Sensor Netw.*, vol. 2014, Jul. 2014, Art. no. 786154.
[4] J. Potter, J. Alves, D. Green, G. Zappa, I. Nissen, and K. McCoy, "The JANUS underwater communications standard," in *Proc. Underwater Commun. Netw. (UComms)*, Sep. 2014, pp. 1–4.
[5] M. Stojanovic, "Recent advances in high-speed underwater acoustic communications," *IEEE J. Ocean. Eng.*, vol. 21, no. 2, pp. 125–136, Apr. 1996.
[6] B. Dushaw, "The acoustic thermometry of ocean climate (ATOC) project: Towards depth-averaged temperature maps of the north Pacific ocean," in *Proc. Int. Symp. Acoust. Tomogr. Thermometry*, 1999, pp. 8–9.
[7] M. Stojanovic, "Acoustic (underwater) communications," in *Encyclopedia of Telecommunications*, J. G. Proakis, Ed. New York, NY, USA: Wiley, 2003.
[8] M. Stojanovic, "High-speed underwater acoustic communications," in *Underwater Acoustic Digital Signal Processing and Communication Systems*. New York, NY, USA: Springer, 2002, pp. 1–35.
[9] R. J. Urick, *Principles of Underwater Sound-2*, New York, NY, USA: Tata McGraw-Hill Education, 1975, pp. 99–197.
[10] P. Du, X. Zhu, and Y. Li, "Direct sequence spread spectrum underwater acoustic communication based on differential correlation detector," in *Proc. IEEE Int. Conf. Signal Process., Commun. Comput. (ICSPCC)*, Sep. 2018, pp. 1–5, doi: 10.1109/ICSPCC.2018.8567803.
[11] G. Han, C. Zhang, L. Shu, N. Sun, and Q. Li, "A survey on deployment algorithms in underwater acoustic sensor networks," *Int. J. Distrib. Sensor Netw.*, vol. 9, no. 12, Dec. 2013, Art. no. 314049.
[12] H. S. P. Van Walree and T. Jenserud, "Characterization of overspread acoustic communication channels," in *Proc. 10th Eur. Conf. Underwater Acoust.*, Jul. 2010, pp. 952–958.
[13] T. C. Yang, "Measurements of temporal coherence of sound transmissions through shallow water," *J. Acoust. Soc. Amer.*, vol. 120, no. 5, pp. 2595–2614, Nov. 2006.
[14] L. Freitag, M. Stojanovic, S. Singh, and M. Johnson, "Analysis of channel effects on direct-sequence and frequency-hopped spread-spectrum acoustic communication," *IEEE J. Ocean. Eng.*, vol. 26, no. 4, pp. 586–593, Oct. 2001.
[15] G. Loubet, V. Capellano, and R. Filipiak, "Underwater spread spectrum communications," in *Proc. OCEANS Conf.*, Halifax, NS, Canada, 1997, pp. 574–579.
[16] F. Zhou, B. LlU, D. G. Nie Yang, W. Zhang, and D. Ma, "M-ary cyclic shift keying spread spectrum underwater acoustic communications based on virtual time-reversal mirror," *Sensors*, vol. 19, pp. 3577–3593,2019.
[17] A. W. Lam and S. Tantaratana, "Theory and applications of spread-spectrum systems: A self-study course," *IEEE/EAB Self-Study Course*, vol. 107, pp. 197–202, 1994.
[18] J. Huang, C. He, and Q. Zhang, "M-ary chirp spread spectrum modulation for underwater acoustic communication," in *Proc. IEEE Region 10 Conf. (TENCON)*, Nov. 2005, pp. 1–4.
[19] W. B. Yang and T. C. Yang, "High-frequency FH-FSK underwater acoustic communications: The environmental effect and signal processing," in *Proc. High Freq. Ocean Acoust. Conf.*, vol. 728, 2004, pp. 106–113.
[20] T. C. Yang and W.-B. Yang, "Performance analysis of direct-sequence spread-spectrum underwater acoustic communications with low signal-to-noise-ratio input signals," *J. Acoust. Soc. Amer.*, vol. 123, no. 2, pp. 842–855, Feb. 2008.
[21] E. J. Kaminsky, "Chirp slope keying for underwater communication," in *Proc. SPIE*, vol. 5778, 2005, pp. 894–905.
[22] J. Lee, J. An, H.-I. Ra, and K. Kim, "Long-range acoustic communication using differential chirp spread spectrum," *Appl. Sci.*, vol. 10, no. 24, p. 8835, Dec. 2020.
[23] A. W. Azim, A. Bazzi, R. Shubair, and M. Chafii, "Dual-mode chirp spread spectrum modulation," *IEEE Wireless Commun. Lett.*, vol. 11, no. 9, pp. 1995–1999, Sep. 2022.

[24] P. Zhu, X. Xu, X. Tu, Y. Chen, and Y. Tao, "Anti-multipath orthogonal chirp division multiplexing for underwater acoustic communication," *IEEE Access*, vol. 8, pp. 13305–13314, 2020.
[25] K. G. Kebkal and R. Bannasch, "Sweep-spread carrier for underwater communication over acoustic channels with strong multipath propagation," *J. Acoust. Soc. Amer.*, vol. 112, no. 5, pp. 2043–2052, Nov. 2002.
[26] B. S. Sharif, J. Neasham, O. R. Hinton, and A. E. Adams, "A computationally efficient Doppler compensation system for underwater acoustic communications," *IEEE J. Ocean. Eng.*, vol. 25, no. 1, pp. 52–61, Jan. 2000.
[27] Doppler shift estimation for underwater acoustic signals," *Proc. ACM Int. Conf. Underwater Netw. Syst.*, 2012, p. 27.
[28] O. Rabaste and T. Chonavel, "Estimation of multipath channels with long impulse response at low SNR via an MCMC method," *IEEE Trans. Signal Process.*, vol. 55, no. 4, pp. 1312–1325, Apr. 2007.
[29] J. S. Kim, H. C. Song, W. S. Hodgkiss, and M. Siderius, "Virtual time series experiment (VIRTEX) simulation tool for underwater acoustic communications.," *J. Acoust. Soc. Amer.*, vol. 126, no. 4, p. 2174, 2009.

CHANG-HYUN YOUN received the B.S. degree from the Department of Radio Communication Engineering, Korea Maritime and Ocean University, South Korea, in 2022, where he is currently pursuing the master's degree. His research interests include sonar signal processing, underwater acoustic communications, underwater wireless optical communications, and underwater acoustic source localization.

HYUNG-IN RA received the B.S. and M.S. degrees from the Department of Radio Communication Engineering, Korea Maritime and Ocean University, South Korea, in 2019 and 2022, respectively, where he is currently pursuing the Ph.D. degree. His research interests include sonar signal processing, underwater acoustic communications, underwater wireless optical communications, and underwater acoustic source localization.

KYUNG-WON LEE received the B.S. degree from the Department of Radio Communication Engineering, Korea Maritime and Ocean University, South Korea, in 2023, where he is currently pursuing the master's degree. His research interests include sonar signal processing, underwater acoustic communications, underwater wireless optical communications, and underwater acoustic source localization.

KI-MAN KIM received the B.S., M.S., and Ph.D. degrees in electronic engineering from Yonsei University, Seoul, South Korea, in 1988, 1990, and 1995, respectively. From 1995 to 1996, he was a fellow of the Yonsei Medical Center. In 1996, he joined as a Faculty Member with the Department of Radio Communication Engineering, Korea Maritime and Ocean University, where he is currently a Professor. His research interests include array signal processing, underwater acoustic communication, and source localization.